

# Modelling and Optimal Sizing of Photovoltaic Water Pumping Systems – Sensitivity Analysis

Simon Meunier\*, Loïc Quéval, Arouna Darga, Philippe Dessante, Claude Marchand

Group of electrical engineering - Paris CNRS, CentraleSupélec, Univ. Paris-Sud, Univ. Paris-Saclay, Sorbonne University Gif-sur-Yvette, 91192, France

\*Correspondence: [simon.meunier@supelec.fr](mailto:simon.meunier@supelec.fr)

Lionel Vido

SATIE | Laboratory of Systems & Applications of Information & Energy Technologies  
Univ. of Cergy-Pontoise  
Cergy-Pontoise, 95000, France

Matthias Heinrich

DargaTech SARL  
Ouagadougou, 12BP407, Burkina Faso

Bernard Multon

SATIE | Laboratory of Systems & Applications of Information & Energy Technologies  
ENS Rennes, Univ. of Rennes, CNRS  
Bruz, 35170, France

Judith A. Cherni,

Elvire A. de la Fresnaye  
Centre for Environmental Policy  
Imperial College London  
London, SW7 2AZ, UK

Peter K. Kitanidis

Department of Civil and Environmental Engineering,  
Stanford Univ.  
Stanford, CA 94305, United States

**Abstract** — Recently we have developed a model of photovoltaic water pumping systems (PVWPS) for domestic water access in poor rural areas. In this article, we perform a sensitivity analysis over the 14 parameters of this model. We study how the variation of the parameters value influences the model output and the optimal sizing obtained from the model, for both the dry and the wet season. Results indicate that the peak power of the photovoltaic modules, the efficiency of the motor-pump and the tank volume have the highest impact on the model output. Besides, the parameters which significantly influence the optimal sizing are the position of the water entry in the tank, the position of the stop level of the float switch, the distance between the stop and restart levels of the float switch, the height between the floor and the bottom of the tank, and the static water level in the borehole. Finally, the thermal parameters of the PV modules and the hydraulic losses have a small impact on the model output and on the optimal sizing. This study can be useful to companies, governments and non-governmental organizations which install PVWPS for domestic water access. It can help them to determine the accuracy at which a given parameter has to be known to correctly model or size these systems. It can also allow them to evaluate the robustness of PVWPS sizing to parameters variation with time. Finally, it may guide the choice of components made by PVWPS installers.

**Keywords** — Photovoltaic system; Water Pumping; Sensitivity analysis; Optimization; Seasonality.

## I. INTRODUCTION

Photovoltaic water pumping systems (PVWPS) are a promising solution for improving water access in rural Africa [1, 2]. They are reliable and economically competitive in remote locations [3], and do not emit greenhouse gases during operation [4].

In the past, several models of PVWPS have been developed and some of them were used to perform sensitivity analyses. The input parameters considered for the sensitivity analyses were related to the pumping head [5, 6], the system design and the system cost. System design parameters include the ratio of the system size to its average production [7], the ratio of the water tank volume to the need for water [6], the loss of power supply probability [6] and the minimum water level in the borehole allowed [8]. Cost parameters include investment cost (photovoltaic modules [8, 9, 10, 11] and forage [8]), operational cost [11], and discount and interest rates [12].

However, to the best knowledge of the authors, the influence of many technical parameters of PVWPS, such as the thermal parameters of the photovoltaic (PV) modules and the hydraulic losses, has not been investigated in previous studies. This omission prevents from determining the accuracy at which these parameters have to be determined when modelling and sizing PVWPS. Moreover, it prevents from knowing the robustness of PVWPS sizing to parameters variation with components ageing (e.g. decrease of PV modules performance with time) and evolution of the local environment (e.g. water resources). Finally, it does not allow to evaluate the impact of technological choices (e.g. choice of components) on PVWPS optimal sizing, nor to forecast future performances of PVWPS as technology improves.

In addition, models which were used in sensitivity analyses do not take the water collection profile as an input. This prevents from modelling PVWPS which include a water tank and a controller that stops and restarts the motor-pump depending on the water level in the tank (figure 1) [13, 14]. No sensitivity analyses have therefore been

performed for PVWPS with this architecture, which is nevertheless often used for domestic water supply.

Finally, to our best knowledge, the influence of seasonality on sensitivity analyses results was not evaluated in previous studies, although the operation of PVWPS varies with seasonality.

The first originality of this article is that we evaluate the influence of several technical parameters that were not studied previously. The second originality is that we present a sensitivity analysis on a PVWPS model which takes water collection as an input. We have presented and validated experimentally this model in [13, 14]. This analysis will notably highlight possible simplifications of our model. The third originality is that the sensitivity analysis is performed for both the dry season and the wet season.

The PVWPS model is presented in section II. The parameters used for the sensitivity analysis are detailed in section III. The impact of the parameters variation on model output and on optimal sizing are described in sections IV and V.

## II. PHOTOVOLTAIC WATER PUMPING SYSTEM MODEL

The PVWPS model is detailed in [13]. The model can be applied to PVPWS with the architecture shown in figure 1. The controller regulates the energy provided by the PV modules to the motor-pump. This regulation is carried out according to two set points of the water level in the tank, which is obtained by a float switch. Water is collected at the fountain by the dwellers. The motor-pump set also contains a maximum point tracking (MPPT) controlled inverter. Figure 2 shows the block diagram of the model. The irradiance on the plane of the PV modules  $G_{pv}$ , the ambient temperature  $T_a$  and the water collected at the fountain  $Q_c$  are the model inputs. The water level in the tank  $H_{tk}$  is the model output.

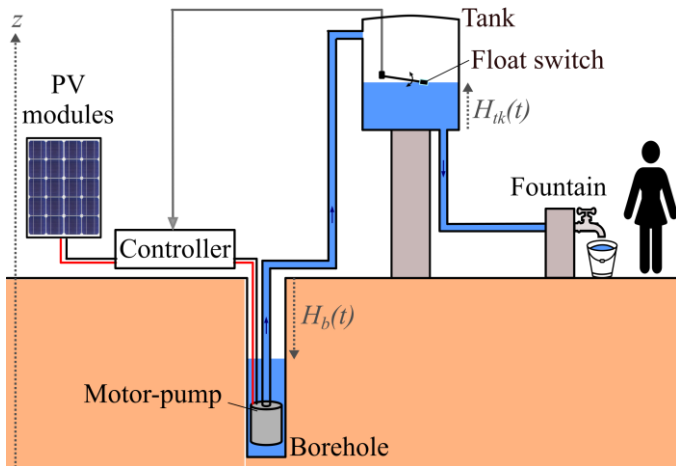


Fig. 1 – Photovoltaic water pumping system architecture.  $H_{tk}$ : water level in the tank;  $H_b$ : water level in the borehole ( $H_b < 0$ ).

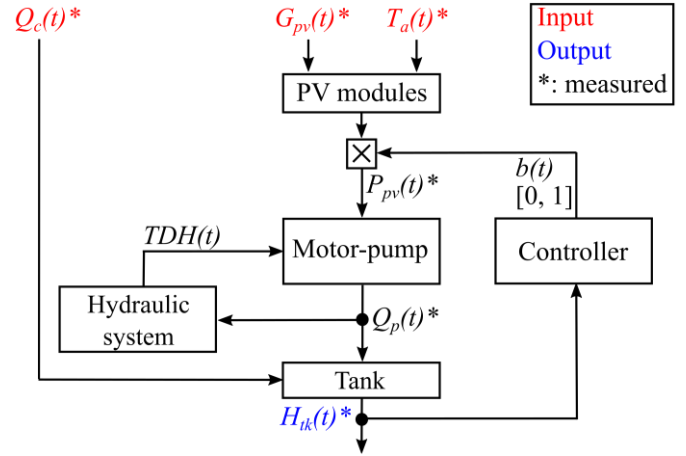


Fig. 2 – Block diagram of the model.  $t$ : time,  $Q_c$ : water collected flow rate,  $G_{pv}$ : irradiance on the plane of the PV modules,  $T_a$ : ambient temperature,  $P_{pv}$ : input power to the motor-pump,  $Q_p$ : pumped flow rate,  $TDH$ : total dynamic head,  $H_{tk}$ : water level in the tank,  $b$ : triggering signal from the controller.

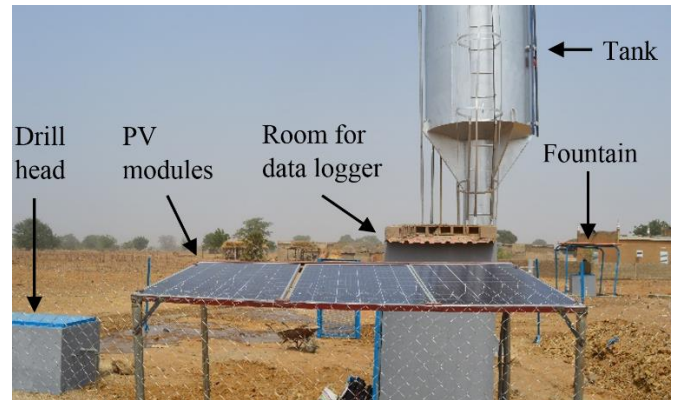


Fig. 3 – Test site: Photovoltaic water pumping system for 250 people in the village of Gogma, Burkina Faso, sub-Saharan Africa.

We have validated the model by using data that we collected on a PVWPS for domestic water access (figure 3) [13]. In this system, there are 620 Wp of multicrystalline PV modules, a motor-pump SQFlex 5A-7 [15] and a cylindrical steel tank of 11.4 m<sup>3</sup>. The quantities measured by our data logger on this system are specified in figure 2. We have been monitoring these quantities with a time step of  $\sim 2.2$  s since January 2018. We rescaled the data to an equally spaced temporal resolution of 1 minute.

Figure 4 and figure 5 present the evolution of the measured irradiance  $G_{pv}$  and the water collected  $Q_c$  for one day of our dataset. Figure 6 shows the pumped flow rate simulated by the model  $Q_p$ . Figure 7, figure 8 and figure 9 present the simulated water level in the borehole  $H_b$ , total dynamic head  $TDH$  and water level in the tank  $H_{tk}$ .  $H_b$  is a component of the total dynamic head  $TDH$ . The variations of  $H_b$ ,  $TDH$  and  $H_{tk}$  are of particular importance in this study, because we have set constraints on them for the optimization (see section V).

By comparing figure 6 and figure 7, we observe that the decrease of the water level in the borehole is due to water pumping. The interruptions of the pumped flow rate (at 11 am for instance) take place when the tank is full (i.e. the water level in the tank  $H_{tk}$  has reached the stop level).  $H_{tk}$  must then go down to the restart level for the pump to resume pumping. When the pumping stops, the water level recovers to the static water level (- 4.9 m). The long and numerous interruptions highlight that the system is oversized in comparison to the water collection.

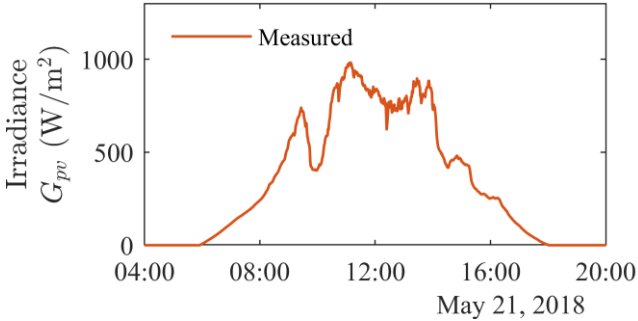


Fig. 4 – Irradiance on the plane of the PV modules – Measured – Model input.

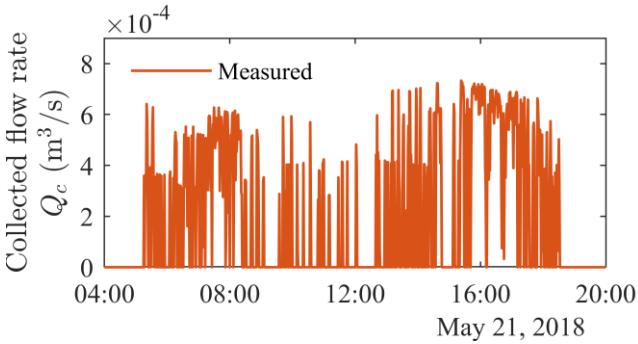


Fig. 5 – Flow rate collected at the fountain – Measured – Model input.

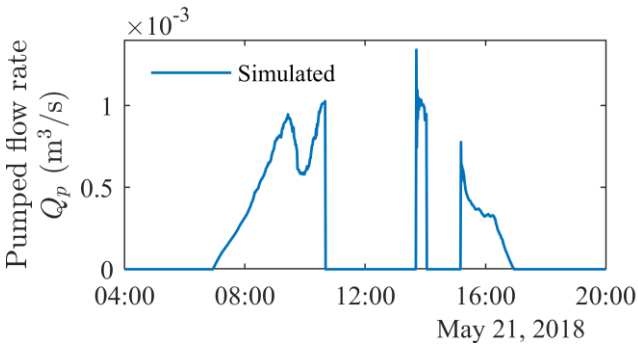


Fig. 6 – Pumped flow rate – Simulated.

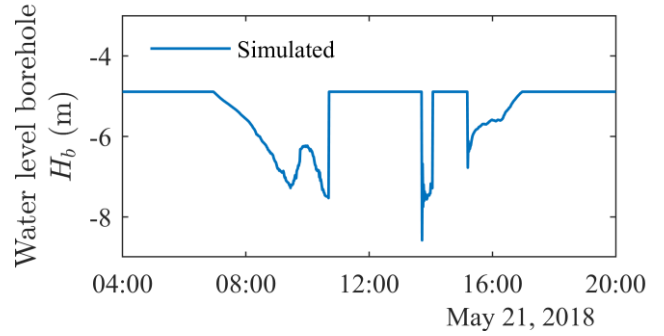


Fig. 7 – Water level in the borehole – Simulated.

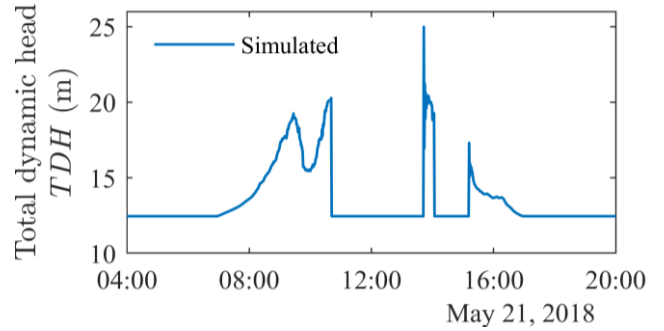


Fig. 8 – Total dynamic head – Simulated.

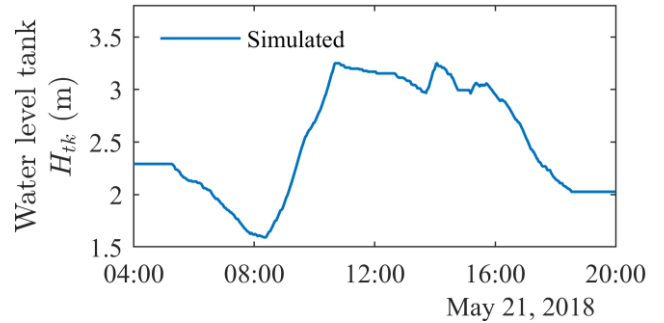


Fig. 9 – Water level in the tank – Simulated – Model output.

### III. SENSITIVITY ANALYSIS PARAMETERS AND METHODOLOGY

The PVWPS model has 14 parameters (table 1) which cover the different parts of the model: PV modules, motor-pump, hydraulic system, tank and controller (figure 2). For Gogma's system, the value of these parameters has been determined by direct measurement, by identification or from the literature [13]. During the sensitivity analysis, these parameters vary around their value in Gogma's system, which is referred to as "reference value".

The sensitivity analysis aims at determining the influence of a variation of the parameters value on the model output and on the optimal sizing. This variation can be due to three main factors: inaccuracy, time and technology.

- 1) *Inaccuracy*. The value of the parameter inputted in the model is different from its real value because of measurement or estimation errors.
- 2) *Time*. The value of the parameter changes due to ageing and/or evolution of the local environment (e.g. water resources). This factor is relevant given the long lifetime of PVWPS, 20 years [16]. For instance, due to ageing, the efficiency of PV modules  $\eta_{STC}$  decreases of between 0.1 and 2 % per year [17].
- 3) *Technology*. The value of the parameter changes with the technology of the corresponding component. For instance, the nominal operating cell temperature

*NOCT* of PV modules varies from one PV technology to another and future PV technologies may have different *NOCT* values than current ones [18].

In this article, we consider a variation of the parameters of table 1 of  $\pm 10\%$  and  $\pm 50\%$  around their reference value *RV*. The new value of the parameter (*NV*) after a variation *s* is therefore:

$$NV = RV(1 + s) \text{ with } s = -10\%, 10\%, -50\%, 50\% \quad (1)$$

In the case of the 16 coefficients of the motor-pump  $k_{m,n}$ , they are all affected by the sensitivity at the same time. This corresponds to modifying the efficiency of the motor-pump.

TABLE 1 – PVWPS MODEL PARAMETERS

Parameter	Description	Sub-model	Way of obtaining the parameter in Gogma	Reference value	Factor(s) that may cause parameter variation
<i>NOCT</i>	Nominal operating cell temperature	PV modules (thermal)	Identification	32 °C	Inaccuracy, Time, Technology
$\beta$	Coefficient of loss due to PV modules temperature	PV modules (thermal)	Literature	- 0.004 °C <sup>-1</sup>	Inaccuracy, Time, Technology
$P_{pv,p}$	Peak power of the PV modules in standard test conditions (STC). $P_{pv,p} = G_0 \eta_{STC} S_{pv}$ where, $G_0$ is the reference irradiance (1000 W/m <sup>2</sup> ), $\eta_{STC}$ is the efficiency of the PV modules in STC, and $S_{pv}$ is the total surface covered by the cells of the PV modules (useful surface).	PV modules (electrical)	Identification for $\eta_{STC}$ , Measure for $S_{pv}$	620 Wp	Inaccuracy, Time, Technology
$k_{m,n}$	Coefficients of the polynomial which fits the characteristic surface of the motor-pump [15]. These coefficients allow to deduce the pumped flow rate $Q_p$ from the input power to the motor-pump $P_{pv}$ and the total dynamic head <i>TDH</i> .	Motor-pump	Datasheet and fitting	16 coefficients	Inaccuracy, Time, Technology
$S_{tk}$	Area of the base of the cylindrical tank	Tank	Measure	3.3 m <sup>2</sup>	Inaccuracy
$H_{tk,c}$	Height of the cylindrical tank	Tank, Controller, Hydraulic system	Measure	3.5 m	Inaccuracy
$H_{tk,i}$	Height between the top of the tank and the water entry in the tank	Tank, Controller, Hydraulic system	Measure	- 0.1 m	Inaccuracy
$H_{tk,s}$	Height between the water entry and the stop controller level	Tank, Controller	Measure	- 0.1 m	Inaccuracy
$H_{tk,r}$	Height between the stop controller level and the restart level	Controller	Measure	- 0.3 m	Inaccuracy
$H_{tk,b}$	Height between the floor and the bottom of the tank	Hydraulic system	Measure	4.2 m	Inaccuracy
$H_{b,s}$	Height between the floor and the static water level in the borehole	Hydraulic system	Identification	- 4.9 m	Inaccuracy, Time
$\kappa_0$	Aquifer losses coefficient	Hydraulic system	Identification	2.0 10 <sup>3</sup> s/m <sup>2</sup>	Inaccuracy, Time
$\mu_0$	Borehole losses coefficient	Hydraulic system	Identification	5.8 10 <sup>5</sup> s <sup>2</sup> /m <sup>5</sup>	Inaccuracy, Time, Technology
$\nu$	Pipe pressure losses coefficient	Hydraulic system	Identification	4.9 10 <sup>6</sup> s <sup>2</sup> /m <sup>5</sup>	Inaccuracy, Time, Technology

Two periods of two weeks are considered in the following. The first period lasts from the 16<sup>th</sup> of May to the 29<sup>th</sup> of May 2018 and is representative of the dry season. The second period lasts from the 29<sup>th</sup> of July to the 11<sup>th</sup> of August 2018 and is representative of the wet season. The average irradiance during the dry and wet seasons are similar but daily water collection at the system is much higher during the dry season (~10 m<sup>3</sup>/day) than during the wet season (~5 m<sup>3</sup>/day).

#### IV. SENSITIVITY ANALYSIS : INFLUENCE ON MODEL OUTPUT

In this section, we study the effect of the variation of the parameters on the PVWPS model output, i.e., the water level in the tank  $H_{tk}$ . For the dry season, for each parameter and for each variation of the parameter, we:

- 1) simulate the water level in the tank during the considered two-week period
- 2) compute the normalized root mean square error  $NRMSE$  on the water level in the tank:

$$NRMSE = \frac{1}{H_{tk,c}} \sqrt{\frac{\sum_{i=1}^n (H_{tk,var}(i) - H_{tk,ref}(i))^2}{n}}$$

where  $H_{tk,c}$  is the height of the tank,  $H_{tk,var}$  is the water level simulated with the variation of the parameter,  $H_{tk,ref}$  is the reference water level (obtained with the reference value of the parameters),  $n$  is the number of points.

The results are presented in figure 10. The same methodology is applied for the wet season and the results are given in figure 11.

Results indicate that the thermal parameters of PV modules  $NOCT$  and  $\beta$ , the heights  $H_{tk,i}$ ,  $H_{tk,s}$ ,  $H_{tk,r}$ ,  $H_{tk,b}$  and  $H_{b,s}$  and the hydraulic losses  $\kappa_0$ ,  $\mu_0$  and  $\nu$  have a small impact on the model output. In addition, for the height of the tank  $H_{tk,c}$ , the NRMSE on the model output is nearly equal to the variation of  $H_{tk,c}$ . Indeed, a change in  $H_{tk,c}$  leads to a continuous offset on the simulated water level in the tank. This variation with  $H_{tk,c}$  is therefore caused by the definition of the parameters describing the tank geometry. Finally, the peak power of the PV modules  $P_{pv,p}$ , the “efficiency” of the motor-pump  $k_{m,n}$  and the surface of the water tank  $S_{tk}$  have the highest impact on the model output. Indeed,  $P_{pv,p}$  and  $k_{m,n}$  strongly influence the pumped flow rate  $Q_p$  and  $S_{tk}$  changes the water tank volume.

Finally, we observe by comparing figure 10 to figure 11, that the variation of the parameters has a lower effect on the NRMSE for the wet season than for the dry season.

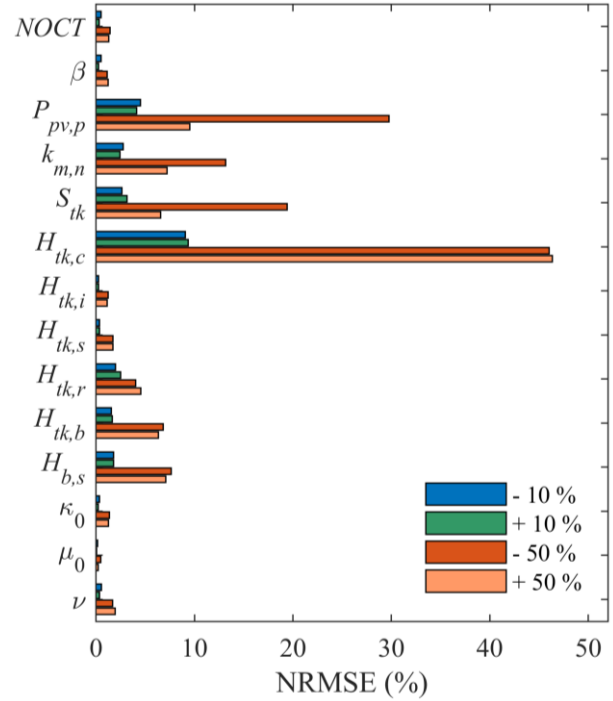


Fig. 10 – Influence of the parameters value on the NRMSE on the simulated water level in the tank  $H_{tk}$ . Dry season (16<sup>th</sup> to the 29<sup>th</sup> of May 2018).

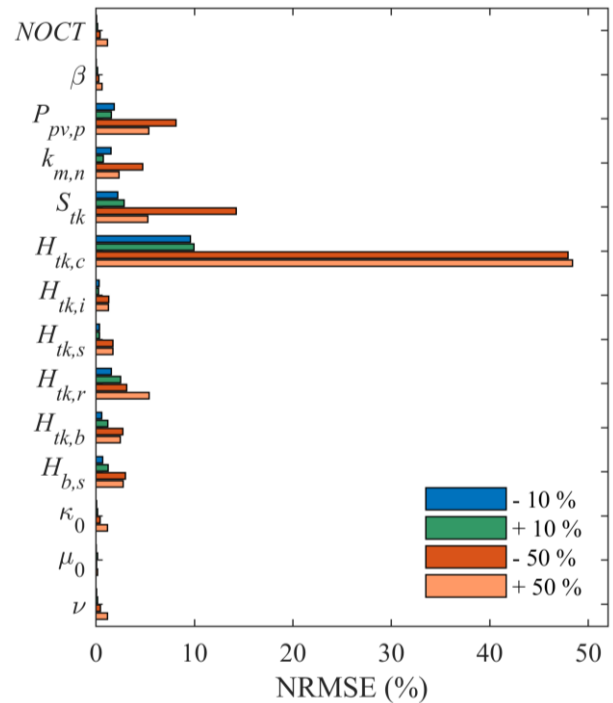


Fig. 11 – Influence of the parameters value on the NRMSE on the simulated water level in the tank  $H_{tk}$ . Wet season (29<sup>th</sup> of July to the 11<sup>th</sup> of August 2018).

## V. SENSITIVITY ANALYSIS: INFLUENCE ON OPTIMAL SIZING

### A. Optimal Sizing

In this section, we study the effect of the variation of the parameters on the optimal sizing of PVWPS. The variables of the optimization are the peak power of the PV modules  $P_{pv,p}$ , the motor-pump number  $MP_i$  and the steel tank volume  $V_{tk}$ . We have digitized the characteristic curves of 8 submersible SQFlex motor-pumps from Grundfos, which are adapted to photovoltaic water pumping and to the characteristics of our case study site [19]. Each motor-pump is associated to a number  $MP_i$ . This choice of variable can be justified by the fact that parameters related to the PV modules, the motor-pump and the tank have the most significant impact on the model output (see section IV). The objective function is the lifecycle cost of the system  $LCC$  in k\$ [16]:

$$LCC = CAPEX + \sum_{j=1}^L \frac{OPEX(j)}{(1+r)^j} \quad (2)$$

where

$$CAPEX = 0.00085 P_{pv,p} + C(MP_i) + 0.76 V_{tk} \quad (3)$$

and

$$OPEX(j) = \begin{cases} \frac{CAPEX}{100} & \text{if } j \neq 10 \\ \frac{CAPEX}{100} + C(MP_i) & \text{if } j = 10 \end{cases} \quad (4)$$

where  $L$  is the lifetime of the PVWPS,  $r$  is the discount rate and  $C(MP_i)$  is the cost of the motor-pump number  $MP_i$  ( $i \in \{1, \dots, 8\}$ ). The discount rate  $r$  is taken equal to 5.6 % and the lifetime  $L$  to 20 years. During this lifetime, it is assumed that the only component that is replaced is the motor-pump, which is changed after 10 years. The coefficients in equations (3) and (4) have been obtained by using cost data provided by companies located in Burkina Faso. Additionally, the cost of the SQFlex motor-pumps considered is given in [19]. It is important to note that there is nearly no variation in the cost of the different motor-pumps. We do not include the fixed part of the  $LCC$  (e.g. cost of drilling the borehole) in the objective function as it does not impact the optimization results. The first constraint of the optimization is that the water level in the tank  $H_{tk}$  (figure 1) must remain higher than zero, in order to fulfil the water needs of the inhabitants. The second constraint is that the water level in the borehole  $H_b$  (figure 1) must not drop below -20 m, in order to prevent the motor-pump from running dry. Indeed, the motor-pump is immersed at -30 m and we set a 10 m safety margin in order to account for hydrological change with time [20]. The third constraint is that, for each motor-

pump  $MP_i$ , the total dynamic head  $TDH$  must remain lower than the maximum pumping height  $H_{p,max}(MP_i)$  specified in the datasheet of the motor-pump. Indeed, the operation of the motor-pump for higher heights is unknown. The PVWPS model is necessary to verify these three constraints. Consequently, it is at this stage that the values of the parameters have an influence. We use a differential evolution algorithm for this optimization and the optimization flow chart is presented in figure 12 [21]. We tested the influence of the optimization algorithm parameters, such as the number of individuals, on the results.

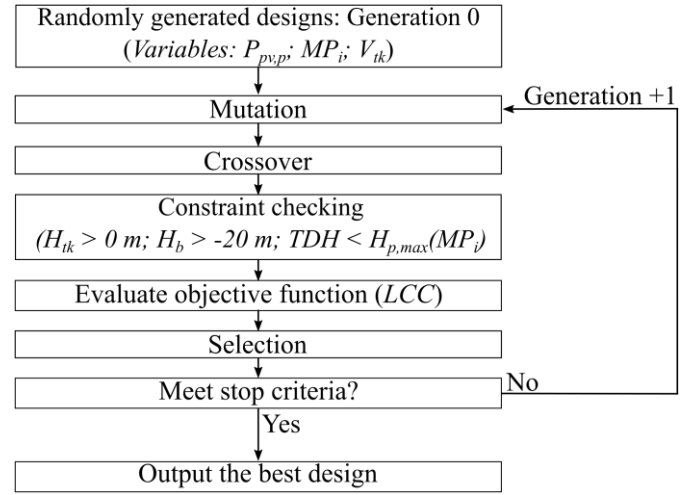


Fig. 12 – Flowchart of the optimization procedure for PVWPS sizing.

We start by performing the optimization for the reference values of the parameters. The optimal value of the  $LCC$  obtained is referred to as the “reference  $LCC$ ”,  $LCC_{ref}$ . This optimization is performed for the periods representative of the dry season and the wet season. The optimal reference  $LCC$  and the associated values of the variables are presented in table 2. The optimal PVWPS is larger for the dry season (higher  $LCC_{ref}$ ) than for the wet one. This is due to the larger water collection by the inhabitants during the dry season (cf section IV). These results can be compared to the current sizing of the system ( $P_{pv,p} = 620$  Wp,  $MP_i =$  SQFlex 5A-7, and  $V_{tk} = 11.4$  m<sup>3</sup>) which is associated to a  $LCC$  of 13.9 k\$.



TABLE 2 – OPTIMIZATION RESULTS WITH THE REFERENCE VALUES OF THE PARAMETERS

	Dry season (16 <sup>th</sup> to 29 <sup>th</sup> of May 2018)	Wet season (29 <sup>th</sup> of July to 11 <sup>th</sup> of August 2018)
$LCC_{ref}$ (k\$)	7.0	6.3
$P_{pv,p}$ (Wp)	850	590
$MP_i$	SQFlex 2.5-2 [22]	SQFlex 2.5-2 [22]
$V_{tk}$ (m <sup>3</sup> )	3.0	2.4

### B. Sensitivity Analysis

As in section IV, we consider a variation of the parameters of table 1 of  $\pm 10\%$  and  $\pm 50\%$  around their reference value. The effect of the variation of the parameters related to the peak power of the PV modules  $P_{pv,p}$ , to the motor-pump  $k_{m,n}$  and to the tank volume ( $S_{tk}, H_{tk,c}$ ) on the optimal sizing is not investigated, as these parameters are related to the variables of optimization. This highlights the interest of the previous study (section IV) to investigate the influence of these parameters. For the dry season, for each parameter and for each variation of the parameter, we:

- 1) perform the optimization and find the optimal  $LCC$
- 2) compute the normalized error on the optimal  $LCC$ ,  $\Delta LCC$ :

$$\Delta LCC = \frac{LCC_{var} - LCC_{ref}}{LCC_{ref}}$$

where  $LCC_{var}$  is the optimal  $LCC$  obtained with the variation of the parameter, and  $LCC_{ref}$  is the reference  $LCC$  (table 2)

The results are presented in figure 13. The same methodology is applied for the wet season and the results are given in figure 14. These figures also show the sign of the variation of the  $LCC$  in response to the variation of the parameter. For instance, for the dry season (figure 13), a variation of  $-50\%$  of the static water level in the borehole  $H_{b,s}$ , decreases the distance between the floor and the static water level and tends to undersize the system ( $\Delta LCC = -2.3\%$ ).

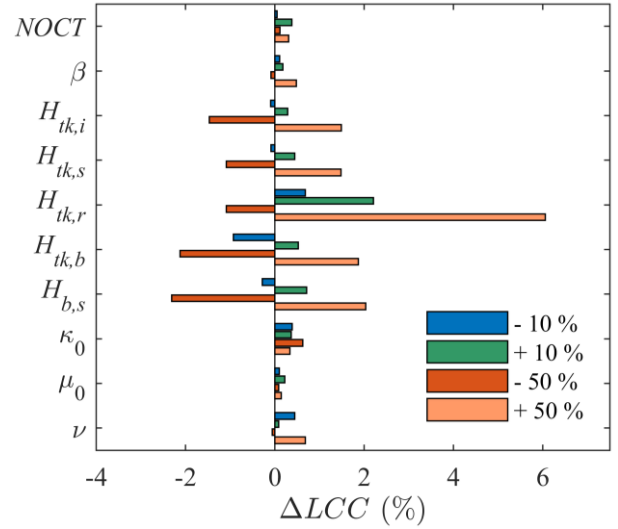


Fig. 13 – Influence of the system parameters values on optimal sizing. Dry season (16<sup>th</sup> to 29<sup>th</sup> of May 2018).

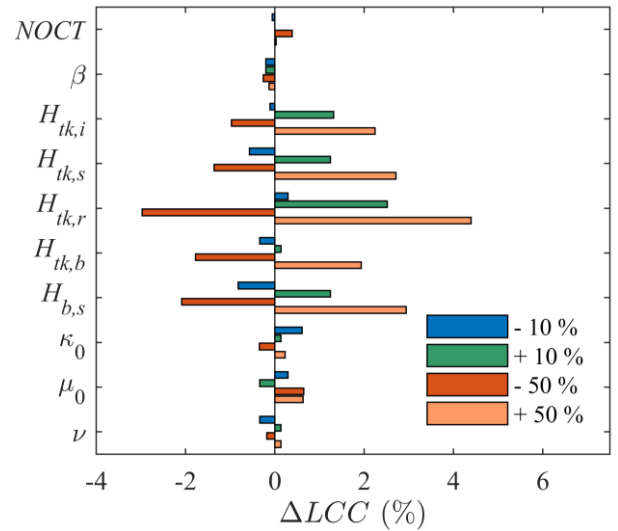


Fig. 14 – Influence of the system parameters values on optimal sizing. Wet season (29<sup>th</sup> of July to 11<sup>th</sup> of August 2018).

Results indicate that the thermal parameters of the PV modules  $NOCT$  and  $\beta$ , and the hydraulic losses  $\kappa_0$ ,  $\mu_0$  and  $\nu$  have a small impact on the optimal sizing. We also observe that the heights  $H_{tk,i}$ ,  $H_{tk,s}$ ,  $H_{tk,r}$ ,  $H_{tk,b}$  and  $H_{b,s}$  have a larger impact on the optimal sizing.  $H_{tk,i}$  is the height between the top of the tank and the water entry in the tank ( $H_{tk,i} < 0$ ).  $H_{tk,s}$  is the height between the water entry and the stop controller level ( $H_{tk,s} < 0$ ). A variation of  $H_{tk,i}$  or  $H_{tk,s}$  influences the percentage of the total tank volume that is available for storing water. For instance, a variation of  $-50\%$  of  $H_{tk,i}$  or  $H_{tk,s}$  increases this percentage and therefore decreases the  $LCC$ .  $H_{tk,r}$  corresponds to the height between the stop controller level and the restart level ( $H_{tk,r} < 0$ ). It sets the water level at which the pump will restart after being stopped due to the tank filling. For

instance, a variation of -50% of  $H_{tk,r}$  allows the motor-pump to restart earlier, to increase the use factor of the motor-pump and therefore to lower the *LCC*.  $H_{tk,b}$  represents the height between the floor and the bottom of the tank ( $H_{tk,b} > 0$ ). A variation of -50% of  $H_{tk,b}$  decreases the total dynamic head *TDH* and therefore allows increasing the pumped flow rate  $Q_p$  for the same input power  $P_{pv}$  to the motor-pump. This explains why the *LCC* decreases.  $H_{b,s}$  represents the static water level in the borehole ( $H_{b,s} < 0$ ). A variation of -50% of  $H_{b,s}$  also decreases the total dynamic head *TDH* and therefore the *LCC*. This result shows that it is important to take into account the evolution of the static water level with time when sizing PVWPS. The static water level may vary of up to several dozen meters during the 20 years lifetime of a PVWPS [20].

We observe that the results of the sensitivity analysis on optimal sizing vary with the simulation period (dry or wet season). Additionally, a comparison of figure 13 and figure 14 to figure 10 and figure 11 reveals that the model output is more sensitive to parameters variation than the optimal sizing.

## VI. CONCLUSION

In this study, we first highlighted the parameters necessary for modeling PVPWS for domestic water access and the factors that may lead to the variation of these parameters. These factors are the inaccuracy of estimation, the variation in time through ageing and evolution of the local environment, and the technology (use a component instead of another one and evolution of the technology with time). Then we investigated the impact of a variation ( $\pm 10\%$  and  $\pm 50\%$ ) of each parameter on the PVWPS model output and optimal sizing.

Results indicate that the peak power of the PV modules  $P_{pv,p}$ , the efficiency of the motor-pump  $k_{m,n}$ , and the surface of the tank  $S_{tk}$  have the highest impact on the model output. They are therefore interesting choices of optimization variables for PVWPS for domestic access. Besides, the parameters which have a large impact on optimal sizing are the height between the top of the tank and the water entry in the tank  $H_{tk,i}$ , the height between the water entry and the stop controller level  $H_{tk,s}$ , the height between the stop and the restart controller level  $H_{tk,r}$ , the height between the floor and the bottom of the tank  $H_{tk,b}$ , and the static water level in the borehole  $H_{b,s}$ . It highlights that these five parameters should be estimated very accurately when installing PVWPS. If it is not the case, then the optimal sizing obtained from the model may in reality not meet the specifications. In addition, it shows that it is important to consider the evolution of the static water level  $H_{b,s}$  over time when sizing a PVWPS. Otherwise, a system

that was sized correctly at year 1 may not meet the specifications at year 20 anymore.

Besides, results show that the thermal parameters of the PV modules *NOCT* and  $\beta$ , and the hydraulic losses  $\kappa_0$ ,  $\mu_0$  and  $\nu$  have a small impact on the model output and on the optimal sizing. The results on *NOCT* and  $\beta$  indicate that it may not be necessary to consider the thermal behavior of PV modules in models of PVWPS for domestic water access. The ambient temperature would then no longer be required as a model input, which simplifies the implementation of the model and reduces the amount of data to collect. Additionally, further studies may be required for hydraulic losses because the error of estimation on these losses may exceed  $\pm 50\%$  in certain cases.

The results of the sensitivity analysis on the model output and on the optimal sizing depend on the considered period (dry and wet season). This suggests that sensitivity analyses should be performed for both the dry and the wet season.

This study can be useful to companies, governments and non-governmental organizations which install PVWPS for domestic water access. First, it can help them to determine the accuracy at which PVWPS parameters have to be determined at the design stage. Second, it can also allow them to evaluate the robustness of PVWPS sizing to parameters change with ageing and evolution of the local environment (notably water resources). Third, it may orientate their choice of components and may allow them to forecast future performances of PVWPS as technology improves. In the future, we will study the influence of the daily average collected flow rate and perform cross sensitivity analyses with selected parameters of the model.

## ACKNOWLEDGMENT

This work is supported by a public grant overseen by the French National research Agency (ANR) as part of the "Investissement d'Avenir" program, through the "IDI 2015" project funded by the IDEX Paris-Saclay, ANR-11-IDEX0003-02.

## REFERENCES

- [1] A. Hmidet, N. Rebei, and O. Hasnaoui, *Experimental studies and performance evaluation of MPPT control strategies for solar-powered water pumps*, in Tenth International Conference on Ecological Vehicles and Renewable Energies (EVER), pp. 1–12, Monte Carlo, Monaco, Apr. 2015
- [2] A. K. Traoré, A. Cardenas, M. L. Doumbia, K. Agbossou, and A. S. H. Maiga, *VHDL description of power management strategy for an autonomous photovoltaic water pumping system for agricultural applications*, in Eleventh International Conference on Ecological Vehicles and Renewable Energies (EVER), pp. 1–8, Monte Carlo, Monaco, Apr. 2016



- [3] B. Singh, A. K. Mishra, and R. Kumar, *Solar Powered Water Pumping System Employing Switched Reluctance Motor Drive*, IEEE Trans. Ind. Appl., vol. 52, no. 5, pp. 3949–3957, 2016.
- [4] S. Ould-Amrouche, D. Rekioua, and A. Hamidat, *Modelling photovoltaic water pumping systems and evaluation of their CO2 emissions mitigation potential*, Appl. Energy, vol. 87, no. 11, pp. 3451–3459, 2010.
- [5] I. Odeh, Y. G. Yohanis, and B. Norton, *Influence of pumping head, insolation and PV array size on PV water pumping system performance*, Sol. Energy, vol. 80, no. 1, pp. 51–64, 2006.
- [6] B. Bouzidi, *New sizing method of PV water pumping systems*, Sustain. Energy Technol. Assess., vol. 4, pp. 1–10, 2013.
- [7] I. Odeh, Y. G. Yohanis, and B. Norton, *Economic viability of photovoltaic water pumping systems*, Sol. Energy, vol. 80, no. 7, pp. 850–860, 2006.
- [8] P. E. Campana, H. Li, J. Zhang, R. Zhang, J. Liu, and J. Yan, *Economic optimization of photovoltaic water pumping systems for irrigation*, Energy Convers. Manag., vol. 95, pp. 32–41, 2015.
- [9] G. Bekele and G. Boneya, *Design of a Photovoltaic-Wind Hybrid Power Generation System for Ethiopian Remote Area*, Energy Procedia, vol. 14, pp. 1760–1765, 2012.
- [10] M. Al-Smailan, *Application of photovoltaic array for pumping water as an alternative to diesel engines in Jordan Badia, Tall Hassan station: Case study*, Renew. Sustain. Energy Rev., vol. 16, no. 7, pp. 4500–4507, 2012.
- [11] M. Montorfano, D. Sbarbaro, and L. Moran, *Economic and Technical Evaluation of Solar-Assisted Water Pump Stations for Mining Applications: A Case of Study*, IEEE Trans. Ind. Appl., vol. 52, no. 5, pp. 4454–4459, 2016.
- [12] B. Bouzidi, M. Haddadi, and O. Belmokhtar, *Assessment of a photovoltaic pumping system in the areas of the Algerian Sahara*, Renew. Sustain. Energy Rev., vol. 13, no. 4, pp. 879–886, 2009.
- [13] S. Meunier, M. Heinrich, J. A. Cherni, L. Queval, P. Dessante, L. Vido, A. Darga, B. Multon and C. Marchand, *Modélisation et validation expérimentale d'un système de pompage photovoltaïque dans une communauté rurale isolée du Burkina Faso*, in Symposium de Génie Electrique (SGE), Nancy, France, July 2018.
- [14] S. Meunier, L. Queval, A. Darga, P. Dessante, C. Marchand, M. Heinrich, J. Cherni, L. Vido, and B. Multon, *Influence of The Temporal Resolution of The Water Consumption Profile on Photovoltaic Water Pumping Systems Modelling and Sizing*, in 7th International Conference on Renewable Energy Research and Applications (ICRERA), pp. 494–499, Paris, France, Oct. 2018.
- [15] Grundfos, “Performance curve of SQFlex 5A-7 motor-pump,” [Online]. Available: <https://product-selection.grundfos.com/product-detail.product-detail.html?custid=GMA&productnumber=95027342&qcid=342768342>.
- [16] E. André de La Fresnaye, *A financial and technical assessment of solar versus hand water pumping for off-grid area – the case of Burkina Faso*, Master dissertation, Imperial College London, United Kingdom, 2018.
- [17] D. C. Jordan and S. R. Kurtz, *Photovoltaic degradation rates - an analytical review*, Prog. Photovolt. Res. Appl., vol. 21, no. 1, pp. 12–29, 2013.
- [18] M. Koehl, M. Heck, S. Wiesmeier, and J. Wirth, *Modeling of the nominal operating cell temperature based on outdoor weathering*, Sol. Energy Mater. Sol. Cells, vol. 95, no. 7, pp. 1638–1646, 2011.
- [19] Off-grid Europe, “Grundfos SQ Flex,” [Online]. Available: <https://www.off-grid-europe.com/accessories/pumps/grundfos/sq-flex>
- [20] A. Rubio-Aliaga, J. M. Sánchez-Lozano, M. S. García-Cascales, M. Benhamou, and A. Molina-García, *GIS based solar resource analysis for irrigation purposes: Rural areas comparison under groundwater scarcity conditions*, Sol. Energy Mater. Sol. Cells, vol. 156, pp. 128–139, 2016.
- [21] K. Price, R. M. Storn, and J. A. Lampinen, *Differential Evolution: A Practical Approach to Global Optimization (Natural Computing Series)*. Secaucus, NJ, USA: Springer-Verlag New York, Inc., 2005.
- [22] Grundfos, “Performance curve of SQFlex 2.5-2 motor-pump,” [Online]. Available: <https://product-selection.grundfos.com/product-detail.product-detail.html?custid=GMA&productnumber=95027330&qcid=465405409>